Crystallization Study on Absorbable Poly(*p*-Dioxanone) Polymers by Differential Scanning Calorimetry

SAŠA ANDJELIĆ, DENNIS JAMIOLKOWSKI, JAMES MCDIVITT, JEROME FISCHER, JACK ZHOU, ROBERT VETRECIN

Ethicon, Inc., A Johnson & Johnson Company, P.O. Box 151, Somerville, New Jersey 08876-0151

ABSTRACT: An investigation was carried out on the crystallization behavior of *p*-dioxanone polymers using differential scanning calorimetry (DSC). Kinetic analyses were performed on data collected primarily during isothermal crystallization. Isothermal data were treated within the framework of the classical Avrami equation. Using this approach, both the Avrami exponent, n, and the crystallization half-time, $t_{1/2}$, were evaluated and their implications are discussed for each system studied. It is shown that a small change in the polymer's composition greatly affects the crystallization kinetics, as well as the crystallizability of the materials. Additionally, nonisothermal crystallization under controlled heating and cooling rates was explored. In the case of cooling from the melt, the Ozawa theory and the recently proposed Calculus method were employed to describe the nonisothermal crystallization kinetics. In view of our results, the validity of these two estimation techniques for determining important kinetic and morphological parameters is also discussed. © 2000 John Wiley & Sons, Inc. J Appl Polym Sci 79: 742–759, 2001

Key words: poly(*p*-dioxanone); absorbable polymers; crystallization; DSC

INTRODUCTION

In an effort to gain a better understanding of the crystallization behavior of absorbable polymers, we have undertaken the development of optimized methodologies and associated characterization techniques for evaluating the crystallization behavior for absorbable materials. It is well documented in the literature[1–5] that the final physical properties and product performances of polymeric medical devices are controlled not only by chemistry, but also by the morphology of the macromolecular chains. A variety of experimental techniques such as dilatometry,[6] differential

scanning calorimetry,[7] X-ray diffraction,[8] hotstage optical microscopy,[9] scanning electron microscopy,[10] dynamic mechanical analysis,[11] dielectric relaxation spectroscopy,[12] light scattering,[13] birefringence,[14] and Raman spectroscopy[15] have been already proven as valuable tools for assessing morphological changes during crystallization. The knowledge gained from these measurements could aid in the understanding of structure–process–property relationships in absorbable synthetic polymers, improve current products and process control, and open up the possibility of producing commercial devices in entirely new areas.

The experimental work in this present investigation was focused on the poly(*p*-dioxanone) homopolymer (PDS) and an 89/11 PDS/glycolide segmented block copolymer.[16] PDS is a synthetic absorbable material, which is typically made by

---

ring-opening polymerization of the lactone mono-mer, *p*-dioxanone (also known as 1,4-dioxanane-2-one).[17] Polymers and copolymers based on *p*-dioxanone have became increasingly important in a variety of biomedical applications[16,18] due to their *in vivo* degradability, low toxicity, softness, and flexibility. For instance, these important features allowed PDS to be made into a synthetic absorbable monofilament suture, with handling characteristics needed by surgeons. It is crucial, however, to control and optimize the morphology of these polymeric devices to provide the best balance of mechanical and biological properties in the final product. A review of the existing litera-ture indicates that no comprehensive study has been performed on the crystallization behavior of this important class of polymers.

The first step in assessing the crystallization data on PDS materials was accomplished by uti-lizing differential scanning calorimetry (DSC). This technique has several advantages including a small sample size, easy-to-handle apparatus, and, more importantly, the ability to achieve a rapid thermal equilibrium, especially at high un-dercooling. Because of these characteristics, DSC has been one of the most convenient and popular methods in studying the crystallization behavior of bioabsorbable polymers (e.g., refs. 19–23 and references therein). Some of the reported studies are of great importance because of their direct relevance to our work and should be singled out. For instance, isothermal crystallization kinetics of biodegradable poly(glycolic acid) (PGA) was studied by Chu using DSC.[24] This work suggested that experimental isotherms of PGA did not agree well with theoretical Avrami prediction through-out the whole crystallization process and that bet-ter fits were observed at higher annealing tem-peratures. Migliaresi and coworkers[20] analyzed the effect of the thermal history on the crystallin-ity of biodegradable poly(L-lactide) (PLLA) poly-mers. They studied the capability of different mo-lecular weight PLLA samples to crystallize under constant heating and cooling rate treatments. While the lower molecular weight polymers devel-oped fair amounts of crystallinity for any cooling rate during cooling from the melt, higher molec-ular weight PLLAs were not able to crystallize when cooled from the melt, unless very low cool-ing rates (0.5 and 1°C/min) were used. When heated after quenching, however, all materials showed similar behavior, with an increase of crys-tallinity as the heating rate decreased. In a sep-arate effort, Urbanovici et al.[22] studied the crys-tallization kinetics of PLLA by DSC under iso-thermal conditions. Kinetic analysis was performed utilizing the classical Avrami equation together with the new model that contains three adjustable parameters. The values of the Avrami exponent, n, were found to be about 3 for both methods, indicating the three-dimensional and athermal growth of the PLLA nuclei. The same conclusion was reached by Iannace and Nicolais[23] in their excellent recent study on isothermal crys-tallization and chain mobility of PLLA. These authors discussed the presence of a fraction of the amorphous phase which does not relax at the glass transition temperature measured by calori-metric and dielectric relaxation spectroscopy (DRS). Interestingly, the amount of this so-called rigid amorphous phase was found to be a function of the annealing temperature. To describe this phenomenon, DRS was a particularly effective tool since the dipoles that were part of the rigid amorphous phase responded by markedly lower mobility (and lower activation energy) than those trapped in a "liquidlike" amorphous part of the molecule.

The principal objective of this communication was to examine the crystallization behavior of PDS materials by DSC. The kinetic data were collected during isothermal and nonisothermal crystallization scans under controlled heating and cooling rates. To evaluate important kinetic/morphological parameters that are characteris-tics of a crystallization process, several known kinetic models were employed.

EXPERIMENTAL

Materials

The majority of data were generated on a dyed PDS homopolymer but a cross-study was per-formed using an undyed homopolymer as well as a 89/11 PDS/glycolide segmented block copoly-mer, whose chemical structure is shown below:
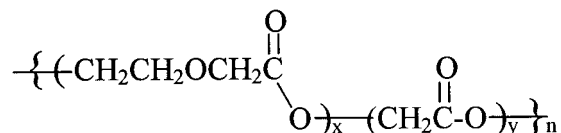
The dye used was D&C Violet No. 2 at approxi-mately 0.2 wt %. Surgical sutures are frequently dyed to aid in their visualization in the surgical site. The dyed and undyed PDS homopolymers

and the copolymer all had weight-average molecular weights of approximately 80,000 as determined by GPC. These three resins displayed inherent viscosities, as determined in hexafluoroisopropanol at 25°C at a concentration of 0.1 g/dL, of 1.85, 1.88, and 1.77 dL/g, respectively. The glass transition temperature of all studied materials was found to be around −10°C, as determined by the DSC method using the heating rate of 10°C/min. The polymers were made in-house by ring-opening bulk polymerization. Due to the high sensitivity of the polymers to hydrolytic degradation, materials were stored and tested under strict dry nitrogen conditions.

Methods

DSC measurements were performed with a TA Instruments differential scanning calorimeter, Model 2910 MDSC, using dry N_2 as a purge gas. The instrument was calibrated with an indium standard for temperature and heat change. Crystallization studies were conducted in three ways: (1) After melting, the sample was cooled under a controlled rate; (2) after melting, the sample was quenched below its glass transition temperature, then heated under a controlled rate; and (3) after melting, the sample was rapidly cooled to a temperature of interest and the crystallization measured under these isothermal conditions.

In a typical nonisothermal crystallization run under a constant heating or cooling rate, a sample weighing around 5 mg was first heated to approximately 35°C above its melting temperature and held in the molten state for 5 min to remove any crystallinity present at that time. From this point, a subsequent cooling step was performed with a constant rate, q, and the crystallization exotherm recorded. In a constant heating rate experiment, the sample was quenched from its amorphous, melted state to below its glass transition temperature, followed by a controlled heating step.

The experiments on the isothermal melt crystallization of PDS homopolymers were carried out as follows: A sample of 5 mg was first melted and maintained for 5 min at 140°C (35°C above its melting point) to remove any nucleation sites present in a sample. Subsequently, tested materials were rapidly cooled (ca. 30°C/min) to the constant test (crystallization) temperature. The isothermal method assumes that no crystallization occurs before the sample reaches the test temperature. Crystallization behavior was char-

acterized over a wide range of temperatures, between 15 and 80°C. The isothermal heat flow curve was integrated to determine the crystallinity as a function of time.

It is worth noting that isothermal and nonisothermal runs were made in randomized order to avoid any bias due to possible molecular weight degradation. All temperature runs for a given polymer were performed on a single sample, and the self-consistency of the data engenders confidence that molecular weight loss during testing is not of any concern.

RESULTS AND DISCUSSION

Isothermal Crystallization

DSC data for the isothermal melt crystallization of dyed PDS over the temperature range of 15–75°C are considered first. A typical DSC thermogram for the crystallization temperature of 40°C is shown in Figure 1. The symmetric shape of the isothermal peak suggests that this process does not contain any secondary crystallization, which is usually accompanied by a long-term heat flow beyond the exothermic maximum.[23] In a few cases, due to a relatively fast crystallization, it was difficult to extrapolate the initial part of the isothermal curve with high accuracy, leading to uncertainty in estimating the value of the zero time. However, this problem does not affect the correct estimation of the kinetic parameters during isothermal measurements.

The evolution of crystallinity with time can be assessed from the degree of crystallization, α, which is expressed by the ratio

$$\alpha = \frac{\Delta H_t}{\Delta H_\infty} = \frac{\int_0^t \frac{dQ}{dt}\, dt}{\int_0^\infty \frac{dQ}{dt}\, dt} \qquad (1)$$

where dQ/dt is the respective heat flow; ΔH_t, the partial area between the DSC curve and the time axis at time t; and ΔH_∞, the total area under the peak and corresponds to the overall heat of crystallization. The degree of crystallization, α, is then the crystalline volume fraction developed at time t.

The kinetic data for isothermal melt crystallization were analyzed using a classical Avrami
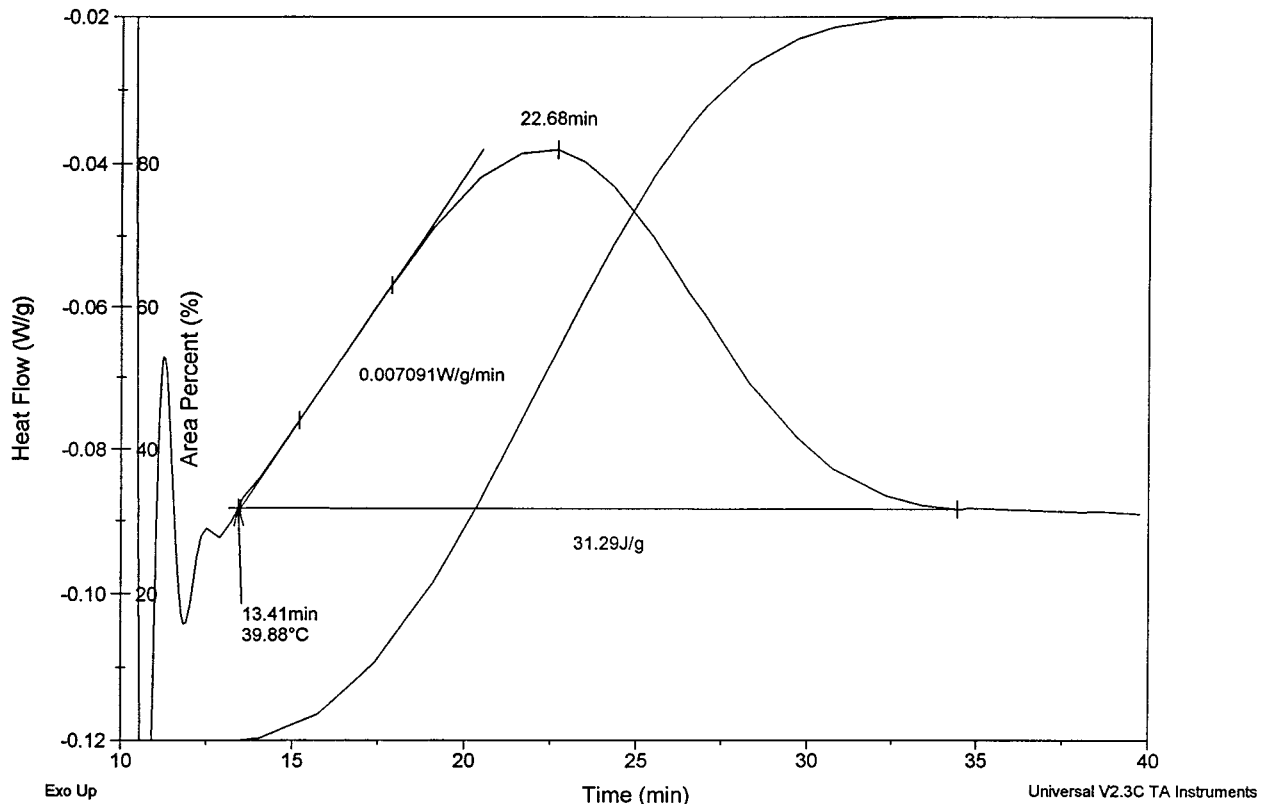
DSC

Figure 1 Isothermal DSC trace, including integrated peak area, obtained during melt crystallization at 40°C.

approach developed six decades ago.[25] According to the Avrami model, the time dependence of α can be described by the following kinetic expression:

$$-\ln(1 - \alpha) = K \times t^n \qquad (2)$$

where K is the composite rate constant, and n, the Avrami exponent, typically ranging from 2 to 4 for semicrystalline polymers. These constants are related to the crystallization half-time, $t_{1/2}$, and to the type of nucleation and geometry of the crystal growth. The crystallization half-time, $t_{1/2}$, is the time needed for crystallinity to reach 50% conversion. The Avrami exponent, n, was determined from the slope of the $\log[-\ln(1 - \alpha)]$ versus $\log t$ curve. Finally, the composite rate constant, K, can be evaluated either from the intercept or calculated using the following expression:

$$K = \frac{\ln 2}{t_{1/2}^n} \qquad (3)$$

In this study, $t_{1/2}$ was determined by fitting each set of data to Eq. (2) and then graphically locating the crystallization time that corresponds to $\alpha = 0.5$. Figure 2 displays both experimentally obtained α versus t data and their best fits (solid lines) originated from the Avrami equation for the isothermal crystallization of the dyed PDS sample at selected crystallization temperatures (T_c). As Figure 2 indicates, an excellent agreement was observed between experimental data and the Avrami theory for all runs except for the two highest crystallization temperatures (70 and 75°C) at the very latest stages of the process. This deviation is manifested by somewhat faster kinetics than predicted, and it was caused, in our opinion, by the onset of secondary crystallization. These data points are marked by arrows in Figure 2. In addition, there are two more signs that may suggest the presence of a secondary process during isothermal melt crystallization of dyed PDS: (1) crystallization exotherms obtained during 70 and 75°C runs are more skewed at the long-term
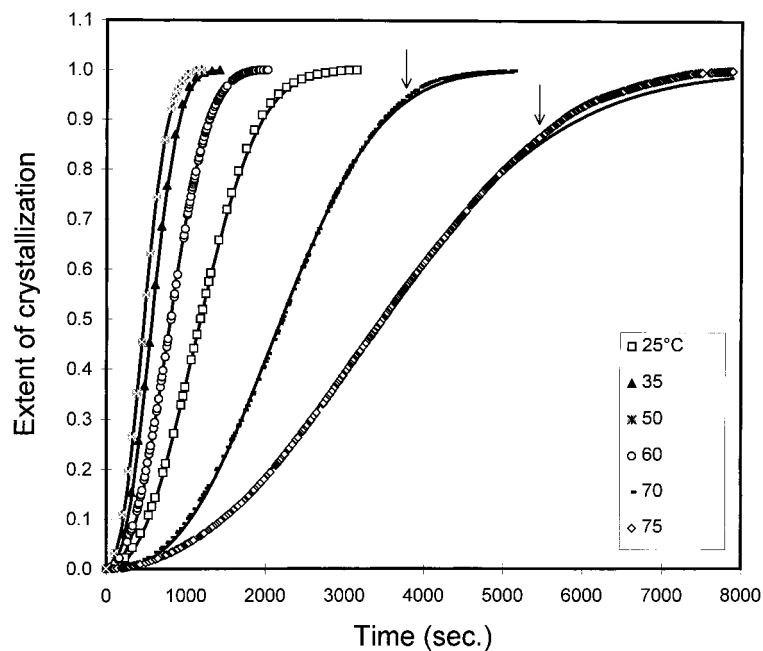
Figure 2 Extent of crystallization as a function of time with annealing temperature as a parameter. Solid lines are fits to the Avrami equation. Arrows indicate the onset of secondary crystallization.

side than what is showed for 40°C in Figure 1, and (2) a significant, 25% increase in the plateau crystallization volume was observed for isothermal crystallization temperatures of 60°C or

higher. This is illustrated in Figure 3, where the heat of crystallization versus time curves are plotted for selected T_c's. The presence of secondary crystallization might be explained by an increase
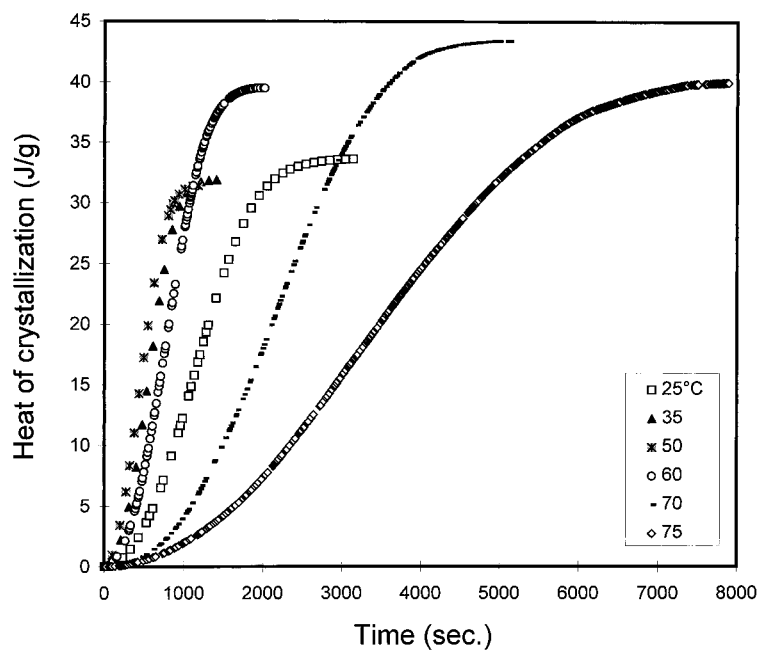

Figure 3 Heat of crystallization as a function of time with crystallization temperature as a parameter.

Table I   Isothermal Crystallization Data for Dyed PDS

T (°C)	$t_{1/2}$ (s)	n	$K(t^{-n})$	ΔH_c (J/g)	Slope (W g^{-1} min^{-1})
20	2100	2.44	5.69e-9	31.5	0.000455
25	1180	2.37	3.74e-8	33.6	0.00161
30	760	2.44	6.48e-8	33.9	0.00384
35	570	2.57	5.73e-8	32.0	0.00666
40	525	2.51	1.03e-7	31.3	0.00709
45	400	2.41	3.71e-7	31.2	0.00886
50	470	2.42	2.37e-7	31.4	0.00870
55	585	2.43	1.31e-7	34.7	0.00665
60	800	2.53	3.24e-8	39.5	0.00408
65	1200	2.62	5.93e-9	40.5	0.00193
70	2200	2.57	1.78e-9	43.4	0.000561
75	3450	2.22	9.70e-9	40.0	0.000202

in the mobility of macromolecular chains due to a lower energy barrier at elevated crystallization temperatures. Additional evidence that would support the existence of this phenomenon in PDS materials was obtained directly from our nonisothermal crystallization studies. These data will be presented and discussed later in the text.

A summary of important kinetic parameters obtained from Figures 1 and 2 are listed in Table I. Analysis of the half-time values indicates that they are a strong function of T_c. The fastest isothermal crystallization rate (the lowest $t_{1/2}$ value) was detected at 45°C. An alternate way to describe crystallization kinetics (not yet seen by the authors in the literature) is to record the initial slope of the crystallization peak (see Fig. 1) for each isothermal run. These data are displayed in Table I (last column) and replotted in Figure 4 with a reciprocal half-time as a function of crystallization temperature for a comparison. A satisfying agreement between these two methods was observed, suggesting that, in at least some cir-
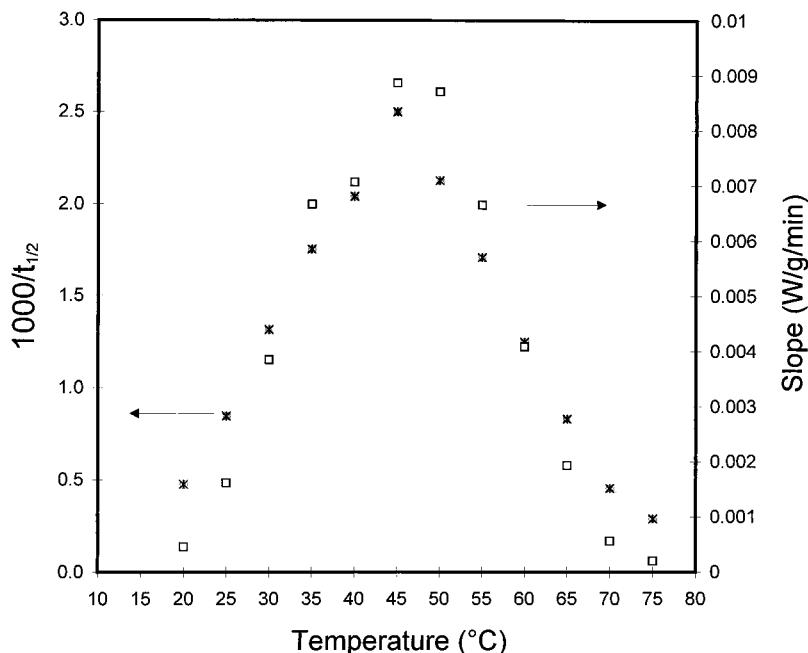

Figure 4   Reciprocal half-time and the left slope of crystallization exotherm as a function of crystallization temperature.
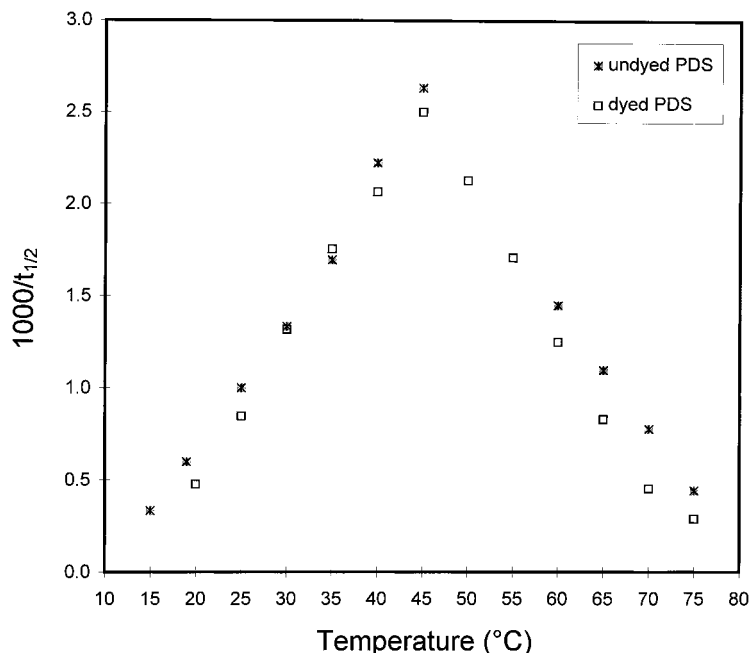
Figure 5 Reciprocal half-time as a function of crystallization temperature for undyed and dyed PDS.

cumstances, the present method can be used to advantage to determine crystallization rates. The main advantage of this approach is that the rates can be established with a shorter experimental time.

Next, we compared the crystallization kinetics of undyed and dyed PDS using $t_{1/2}$ as a kinetic parameter, as shown in Figure 5. For any given isothermal crystallization run, except that performed at 35°C, we found that the crystallization of undyed PDS is slightly faster than that of the dyed. Data collected between 45 and 60°C for undyed PDS are not included in the analysis because at these temperatures crystallization progressed notably before the sample reached thermal equilibrium, causing the distortion of the initial portion of the thermogram. Although small differences in the crystallization kinetics between the undyed and dyed PDS homopolymer cannot be explained at this time (especially that the undyed crystallizes faster), it is apparent that optimum processing conditions for these two materials will be accordingly different.

The geometry of the crystal habit during isothermal crystallization of dyed PDS, expressed via the Avrami exponent, n, is also listed in Table I. For the sake of clarity, these results are graphically displayed in Figure 6. The values of n were relatively constant at 2.5 for all T_c investigated,

indicating that the crystal growth was three-dimensional. The same value was found for the undyed PDS homopolymer. This is in agreement with the results reported earlier for a majority of polyesters,[26,27] including poly(ethylene terephtalate) and poly(ε-caprolactone). With regards to the copolymer, an isothermal crystallization study on the copolymer unfortunately could not be performed using DSC. This was the result of the crystallization rate being so low that the rate of heat gain in the calorimeter was less than was the heat-loss rate resulting in no net change in the enthalpy signal. We expect that supporting evidence from hot-stage optical microscopy measurements would be particularly beneficial to judge the consistency of the Avrami exponent for this group of materials and will be the subject of future investigations.

Nonisothermal Crystallization

Effect of Heating Rate

The second part of this study dealt with nonisothermal crystallization of dyed PDS utilizing controlled heating steps. Samples were quenched from the molten state to obtain a fully amorphous morphology and, subsequently, heated at rates of 1, 2, 4, 8, 15, and 20°C/min.
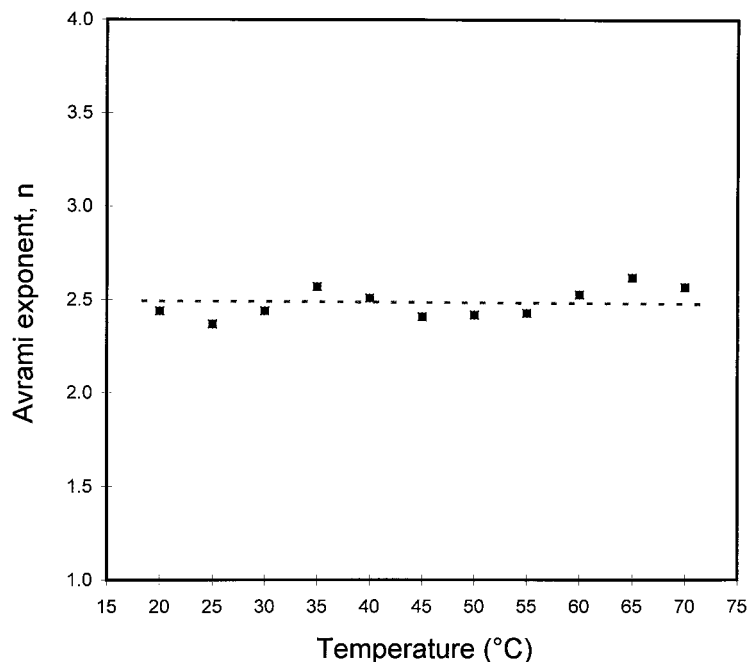
Figure 6 Avrami exponent, n, as a function of crystallization temperature.

A typical DSC trace generated using this method is shown in Figure 7 for the heating rate of 1°C/min. An important feature that emerged from this study is the discovery of two independent crystallization exotherms. The higher-temperature process is assigned to the secondary crystallization that was suggested earlier by the isothermal measurements at elevated temperatures. Table II summarizes most of the thermal data regarding the effect of the heating rate on the crystallization and melting behavior of dyed PDS. With an increase in heating rates, both crystallization exotherms appeared at higher temperatures. A particularly large shift was observed for the primary crystallization peak. The melting point location, on the other hand, was almost constant for the conditions used in this study. It is worth noting that the melting endotherm is characterized by a 10°C shift to lower temperature when compared to that of the initial sample (first heat). This is probably due to the nature of the short annealing treatment that was performed on a sample. Lack of sufficient time for the crystallization to occur during these nonisothermal measurements prevented crystals to fully grow and perfect their morphology. We would like to emphasize that exactly the same effect was observed earlier for PLLA.[20] Additionally, the data in Table II indicate that the peak areas under the secondary crystallization exotherm and the corresponding melting endotherm systematically decreased with increase in the heating rate. We attribute this to the simple fact that the polymeric samples have less time to undergo secondary crystallization as heating rates are increased. Although the primary crystallization peaks increased in temperature as mentioned above, their areas remained fairly constant. This invariance suggests that the same amount of crystallization occurred during this early process within the experimental heating rate range studied. The sum of areas under the T_{c1} and T_{c2} peaks equal roughly those for a fusion process, suggesting that the heating scan started from a fully amorphous sample. Certain discrepancies that are observed for the lower heating rate runs reflect the inability of the instrument to account for a continuing incremental crystallization that took place between the two exotherms during longer-lasting runs.

The areas under the melting peak (heat of fusion) as a function of the heating rate for the undyed and dyed PDS homopolymers along with the copolymer are now compared. With an increase in the heating rate, the apparent heat of melting systematically decreased. This effect is associated to the same concept of the previously stated argument related to the heat-loss and -gain characteristics of the calorimeter. Compensation for induced crystallization in the melting
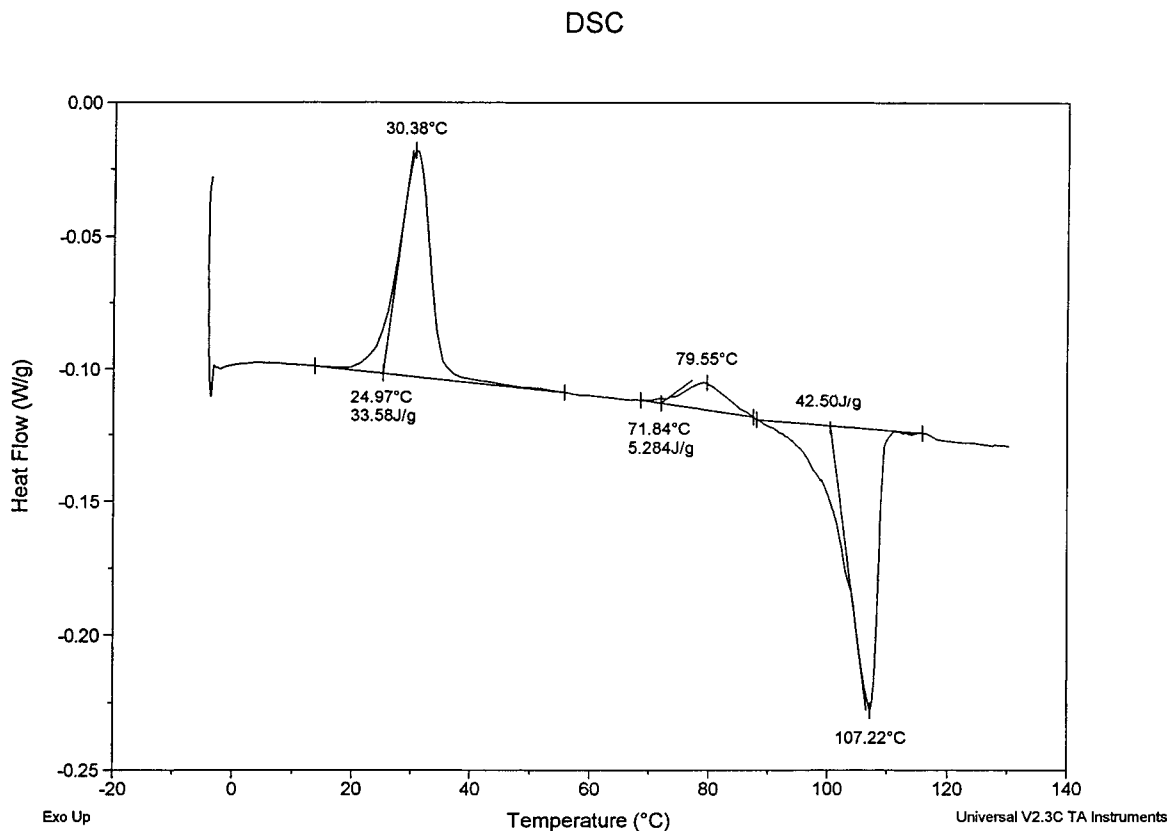
DSC

Figure 7 Nonisothermal DSC trace obtained during heating step from the quenched amorphous state at 1°C/min.

endotherm can only result when an area exists for that event that can be attributed to an enthalpy change. At slow heating rates (i.e., 1–2°C/min), a low crystallization rate does not impart changes to the enthalpy (baseline) of the DSC thermogram, while at higher heating rates (>10°C/min), the secondary crystallization processes do not have time to occur. The observed pattern is graphically illustrated in Figure 8. For any given heating rate, data points for undyed and dyed

PDS practically overlapped, suggesting that an equal crystal content was present at the end of each heating step. The copolymer, however, showed a considerably lower ability to crystallize as was manifested by the small heat of fusion values. In addition, the data in Figure 8 indicate that, in this case, heating rates of 10°C/min or higher did not produce any crystallinity at all; flat DSC thermograms are obtained during nonisothermal measurements at higher heating rates.

Table II   Nonisothermal Crystallization Data Obtained During Constant Heating Rate Experiments for Dyed PDS

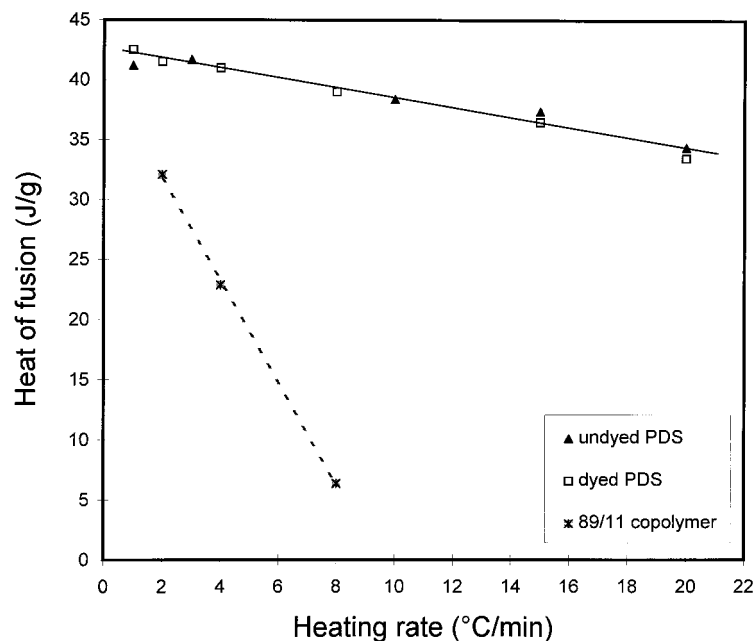| Heating Rate (°C/min)	T_{c1} (°C)	T_{c2} (°C)	T_m (°C)	Peak Area at T_{c1} (J/g)	Peak Area at T_{c2} (J/g)	Peak Area at T_m (J/g)
1	30.4	79.6	107.2	33.6	5.29	42.5
2	35.1	79.7	106.3	34.2	4.78	41.5
4	42.4	82.9	106.0	35.5	4.22	41.0
8	51.7	87.0	105.5	35.6	3.34	39.0
15	59.4	88.5	105.3	35.9	0.50	36.5
20	65.9	—	105.3	33.5	—	33.5

Figure 8 Heat of fusion as a function of heating rate for undyed and dyed PDS homopolymer and undyed copolymer.

Through extrapolation of the curves in Figure 8 to a zero heating rate, one reaches the conclusion that the equilibrium heat of fusion for the copolymer is lower than those of the PDS homopolymers. The reason for this behavior can be found in a disruptive role that glycolic acid comonomer plays in the overall ability of the copolymer's macromolecular chains to align properly for the crystal formation.

Effect of Cooling Rate

The study of morphological changes of absorbable semicrystalline polymers occurring during nonisothermal crystallization from the molten state is of increasing technological importance, because these conditions are the closest to real industrial processing. It is anticipated that the kinetics and extent of crystallization will be grossly affected by the rate at which the polymer is solidified from its fully amorphous molten state. In this section, we analyze the kinetic data using two existing methods, the first one based on the well-known Ozawa equation,[28] followed by the Calculus method recently proposed by Cazé et al.[29]

A typical DSC trace captured during the constant cooling rate experiment is shown in Figure 9 for the dyed PDS sample cooled from the melt at 0.5°C/min. A summary of thermal characteristics obtained by this method is listed in Table III for different cooling rates. With a slower cooling rate, the crystallization exotherm becomes larger and the crystallization temperature, T_c, shifts to a higher value. This behavior is related to the fact that, for slower cooling cycles, the polymer remains for a longer time at a temperature range sufficiently low for the polymer to begin to crystallize, but also high enough to provide sufficient chain mobility to facilitate crystal growth. By cooling the dyed PDS sample at rates faster than 5°C/min, on the other hand, we obtained a supercooled material, freezing the molecular motion quickly before the chains were able to generate ordered crystals. The last column in Table III displays the slope values of the right side of the crystallization exotherm that are shown in Figure 9. These numbers mirror the crystallization rate and, as was graphically illustrated in Figure 10, decreased continuously in a nonlinear fashion with increase in the cooling rate.

To collect information about the crystalline fraction attainable at different cooling rates, we recorded the total area under the crystallization exotherm after series of nonisothermal runs. These results are plotted against different cooling rates in Figure 11 for all the materials under study. A trend was observed: With increase in the cooling rate, the heat of crystallization decreased
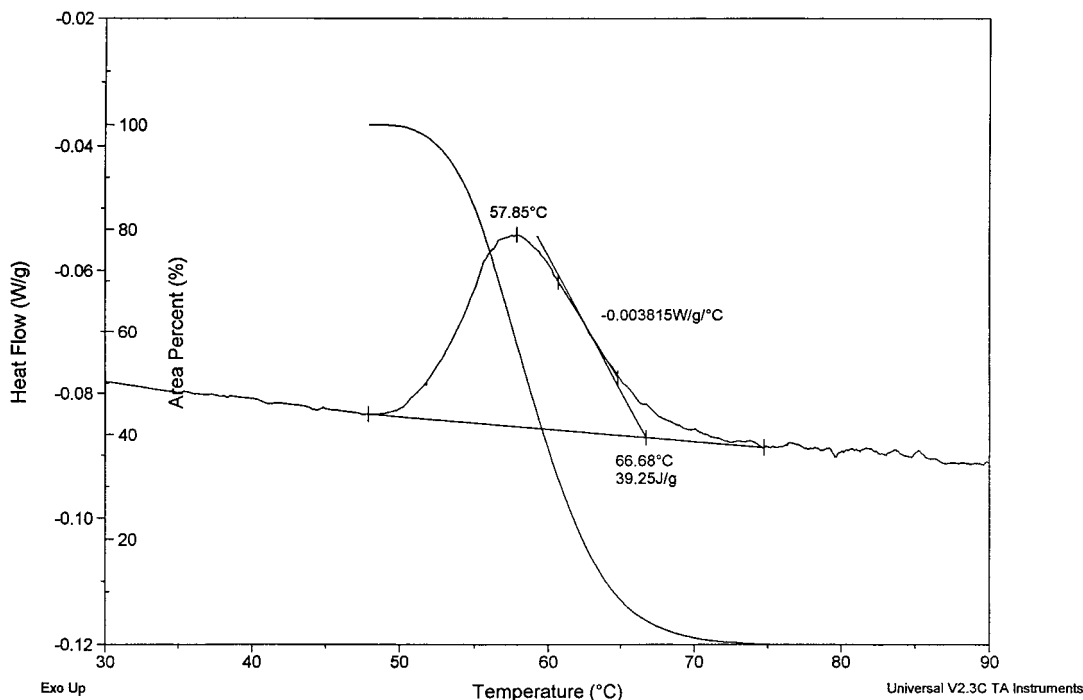
DSC

Figure 9 A nonisothermal DSC trace, including an integrated peak area, obtained during crystallization from the melt at constant cooling rate of 0.5°C/min.

abruptly. However, a remarkably different extent of crystallization is encountered not only between the PDS homopolymers and the copolymer, but also between the undyed and dyed PDS themselves. According to data in Figure 11, for every given cooling rate, the crystalline content in undyed PDS was the highest for the three materials. This finding, obtained under nonisothermal cooling conditions, is in line with the relative crystallization rates observed earlier for the samples under isothermal conditions.

Table III Nonisothermal Crystallization Data Obtained During Constant Cooling Rate Experiments for Dyed PDS

Cooling Rate (°C/min)	T_c (°C)	Peak Area at T_c (J/g)	Slope Value (W g^{-1} °C^{-1})
0.25	64.0	41.2	−0.00416
0.5	57.8	39.3	−0.00381
1	48.4	32.8	−0.00367
2	42.6	14.0	−0.00182
3	39.2	4.0	−0.00109
4	41.3	1.5	−0.00068

Methods

The final part of this study dealt with semiempirical treatments of nonisothermal crystallization kinetics under constant cooling rate conditions according to two proposed methods. The Ozawa approach[28] and the recently developed Calculus method[29,30] were used here to describe the crystallization kinetics of PDS polymers. Both of these methods allow the determination of the type of nucleation (homogeneous or heterogeneous) and characterize the growth geometry (one-, two-, or three-dimensional) using the Avrami exponent, n.

Ozawa Method

Theoretical treatment of the nonisothermal crystallization kinetics was addressed by Ozawa[28] as early as 1971 and represents a modified Avrami approach. The Avrami approach was described and utilized in the previous section for our isothermal studies. The Ozawa method determines the Avrami exponent, n, using data exclusively confined to the primary crystallization regime. There are certain limitations involved, including
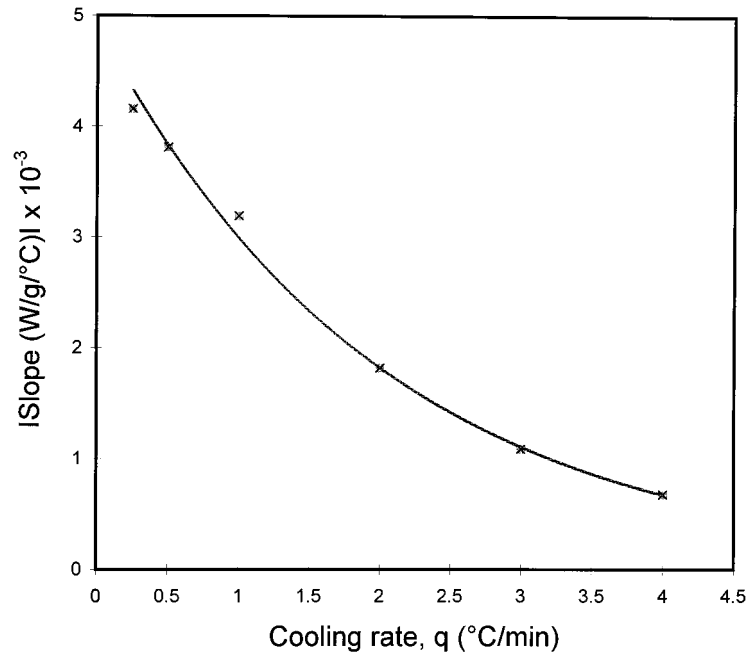
Figure 10 The right-side slope of crystallization exotherm during nonisothermal crystallization as a function of different cooling rates.

the important assumption that n is independent of temperature.

The determination of n during the constant cooling rate steps from the molten state uses the following equation proposed by Ozawa:

$$X_V = 1 - \exp\left(-\frac{f_C}{q^n}\right) \tag{4}$$

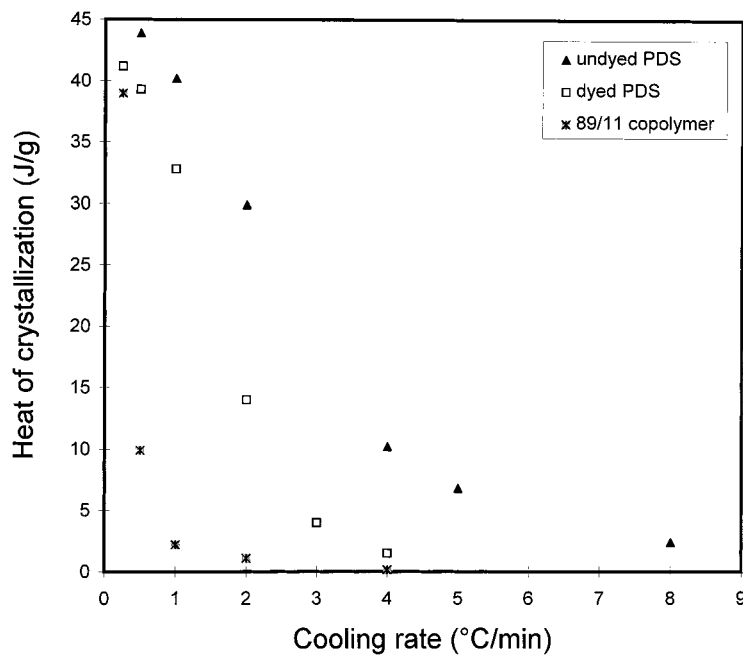where X_V is the volume fraction of the transformed polymer at the temperature T; q, the cool-

Figure 11 Heat of crystallization as a function of different cooling rates for undyed and dyed PDS homopolymer and undyed copolymer.
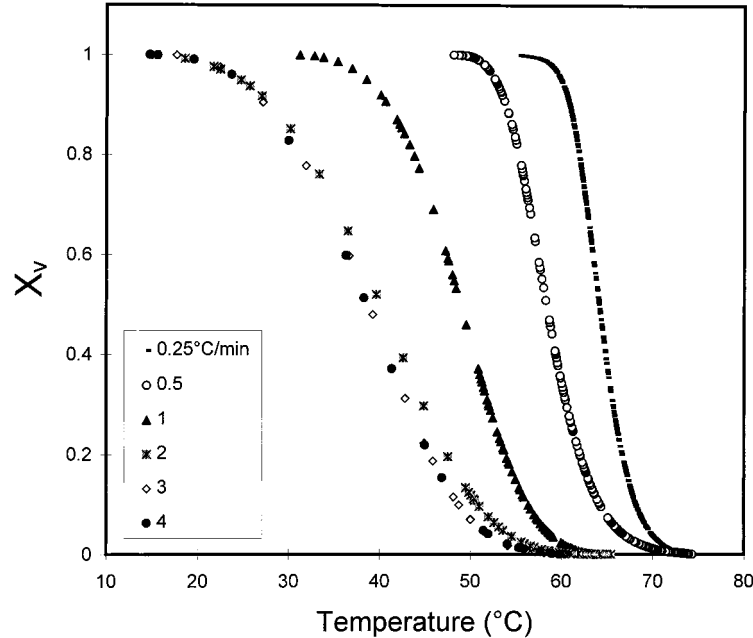
Figure 12 Volume fraction of the transformed polymer, X_V, as a function of temperature with cooling rate as a parameter.

ing rate; n, the Avrami exponent; and f_C, the so-called cooling function, which has been assumed to increase exponentially with temperature. In general, crystallization thermograms obtained in DSC give the transformed mass function X_W by partial integration of the exothermal peak at the temperature T. Since eq. (4) uses a transform volume fraction, it is necessary to first convert X_W into X_V by the following expression:

$$X_V = \frac{X_W \dfrac{\rho_A}{\rho_C}}{1 - \left[1 - \dfrac{\rho_A}{\rho_C}\right] X_W} \qquad (5)$$

where ρ_A and ρ_C are the density of the amorphous and crystallized phases, respectively. As determined by Dolegiewitz,[31] a relationship which ties density and percent crystallinity (using X-ray defraction) for undyed and dyed PDS monofilaments is

$$\rho = 1.3382 + \alpha 1.337 \times 10^{-3} \qquad (6)$$

where α denotes a percent of crystallinity. Combining eqs. (5) and (6), the original DSC curve can be now redrawn as a curve which depends on the transformed volume fraction. In Figure 12, the

nonisothermal crystallization kinetics were displayed by plotting X_V against the temperature for different cooling rates.

To determine the Avrami exponent using the Ozawa method, eq. (4) needs to be rewritten as follows:

$$\ln[-\ln(1 - X_V)] = \ln f_C - n \ln q \qquad (7)$$

Equation (7) involves determination of transformed volume fractions for different cooling rates at a given temperature. Plots of $\ln[-\ln(1 - X_V)]$ versus $\ln(q)$ should result in straight lines with the exponent n calculated from the slope. Due to the considerable change in the degree of supercooling with different cooling rates, it appears difficult, in practice, to find more than a few points at a particular temperature. Results of this analysis generated at three applicable temperatures are presented in Figure 13(A,B) for undyed and dyed PDS. Almost perfect linear dependencies were observed for both systems at all temperatures, suggesting that the Avrami exponent, n, is constant within the selected cooling rate range. However, we detected a systematic change in the slope, increasing with increasing temperature. The calculated Avrami exponents for undyed
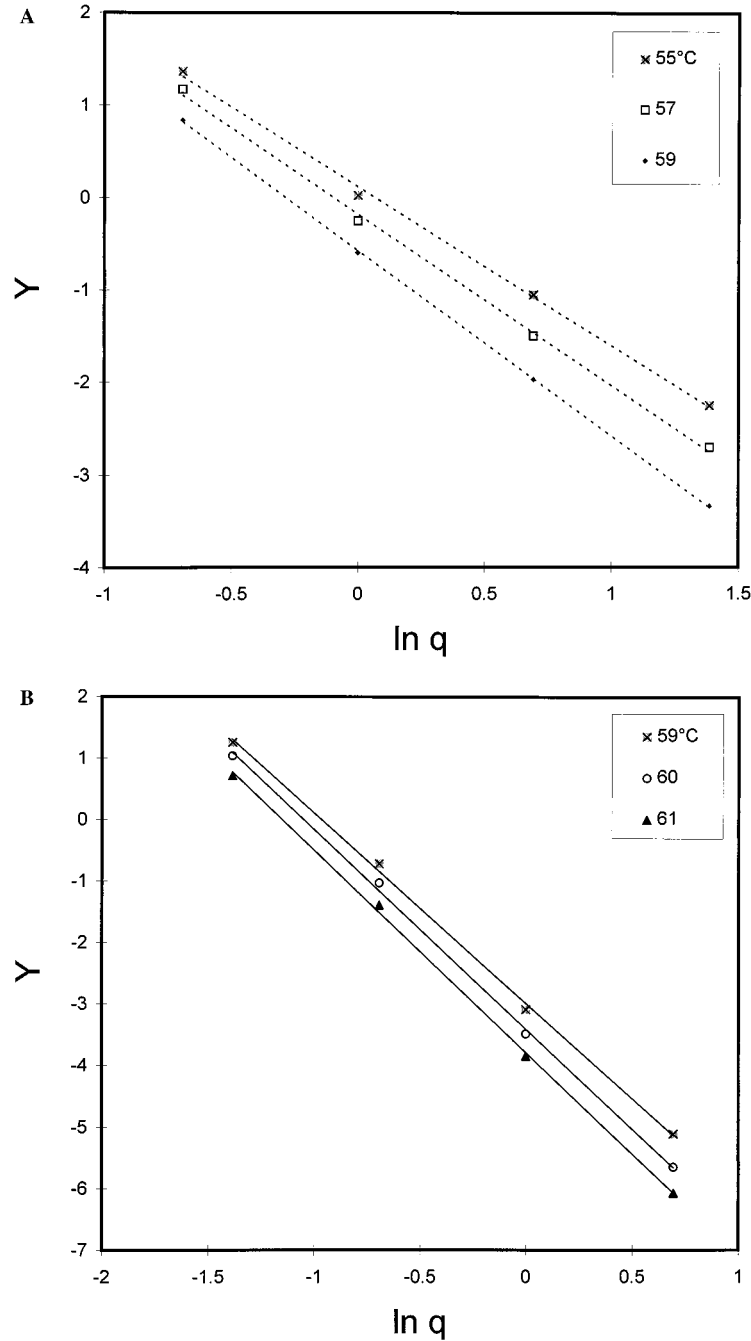
Figure 13   (A) Linear plots of $Y = \ln[-\ln(1 - X_V)]$ against $\ln q$ for undyed PDS at various temperatures. (B) Linear plots of $Y = \ln[-\ln(1 - X_V)]$ against $\ln q$ for dyed PDS at various temperatures.

PDS were 1.72, 1.85, and 2.0 at 55, 57, and 59°C, respectively. According to the literature,[27] n close to 2 may describe heterogeneous nucleation with a two-directional disclike growth. Values of 3.15, 3.31, and 3.37 were obtained at 59, 60, and 61°C, respectively, for dyed PDS and may accompany heterogeneous nucleation with three-dimensional spherulitic growth. These data are difficult to interpret considering the fact that the Avrami exponent 2.5 was found for both polymers during isothermal crystallization. The major obstacle to cor-

rectly interpret these findings using Ozawa's theory rests with his assumption that n is independent of temperature. Clearly, the data show that this is not the case with this family of materials, leading us to believe that the Ozawa method of analysis is not entirely suitable here.

Calculus Method

A modification of the Ozawa method was recently developed by Cazé and coworkers[29] for studying nonisothermal crystallization kinetics during constant cooling steps. This new method is based on the experimental observation that the crystallization exotherms essentially have a Gaussian shape. For this reason, only the maximum and inflection points of the curve need to be considered, substantially simplifying the determination of the Avrami exponent, n. An outline of equations used in this study is briefly recapped below:

Assuming a linear dependence between $\ln f_C$ versus temperature, as suggested by the Ozawa theory, we may write

$$\ln f_C = aT + b \qquad (8)$$

where a and b are empirical constants. Cazé et al. suggested that it is possible to express the value of the extremum of the exothermal curve T_q for a given cooling rate q by finding the zero of the primary derivative of the peak equation:

$$\frac{\partial}{\partial T}\left(\frac{\partial}{\partial T} X_V\right)_q = 0 \qquad (9)$$

Using eq. (4), this equation can be solved as

$$0 = \frac{\partial^2 f_C}{\partial T^2} - \frac{1}{q^n}\left(\frac{\partial f_C}{\partial T}\right)^2 \qquad (10)$$

Substituting derivatives from expression (8) and setting $T = T_q$, the following relationship emerged:

$$T_q = \frac{n}{a}\ln q - \frac{b}{a} \qquad (11)$$

The Avrami exponent, n, is then obtained as the slope of the T_q versus $\ln(q)/a$ curve. To evaluate the constant "a," the following steps were performed. At the extreme point $T = T_q$, combining eqs. (8) and (11) results in

$$f_C(T_q) = q^n \qquad (12)$$

Installing this expression in the Ozawa equation, we finally arrived at

$$\ln[-\ln(1 - X_V)] = a(T - T_q) \qquad (13)$$

Thus, plots of $\ln[-\ln(1 - X_V)]$ versus T allow the calculation of the constant "a" and the product $-aT_q$ from the slope and intercept, respectively. Since eq. (13) is confined to the primary crystallization regime, the above linear regression analysis has to comply with two criteria: (1) the lowest X_V employed should be kept around 2% to ensure precision, and (2) the range of X_V selected should cover data in such a way that the coefficient of determination, r^2, is greater than 0.980. Having that in mind, linear plots of $\ln[-\ln(1 - X_V)]$ against temperature were constructed for undyed and dyed PDS polymers at different cooling rates. X_V data for both systems were taken, approximately, from 2 to 50%. As an example of this calculation, data for dyed PDS are shown in Figure 14. Estimated parameters "a" and T_q obtained from this figure are listed in Table IV. The results show that both absolute "a" (i.e., $|a|$) and T_q increase with decreasing q. Making use of these data, plots of T_q versus $\ln q/a$ were made for undyed and dyed PDS to determine the Avrami exponent n. The data are shown in Figure 15. Unexpectedly, the absence of a single linear curve was observed for both polymers. Instead, we can identify two regions with two distinctly different slopes that characterize lower (region I) and higher (II) cooling rate domains. Avrami exponent values of 3.0 and 1.1 for undyed and 5.2 and 0.75 for dyed PDS were calculated from regions I and II, respectively.

We stress that Chuah et al.,[30] obtained exclusively a single Avrami exponent using this method for a wide variety of semicrystalline polymers including the related polyester, poly(ε-caprolactone). What, then, causes this unique response of PDS materials? We believe that a substantiality lower crystallization rate of undyed and dyed PDS, compared to materials studied in ref. 30, must play a critical role in this event. In the above-mentioned study, Chuah and coworkers used a very broad cooling rate range (from 2 to 40°C/min) to describe fast crystallization behavior for the majority of the polymers tested. We remind the reader that, in our case, the ability of PDS materials to crystallize was drastically re-
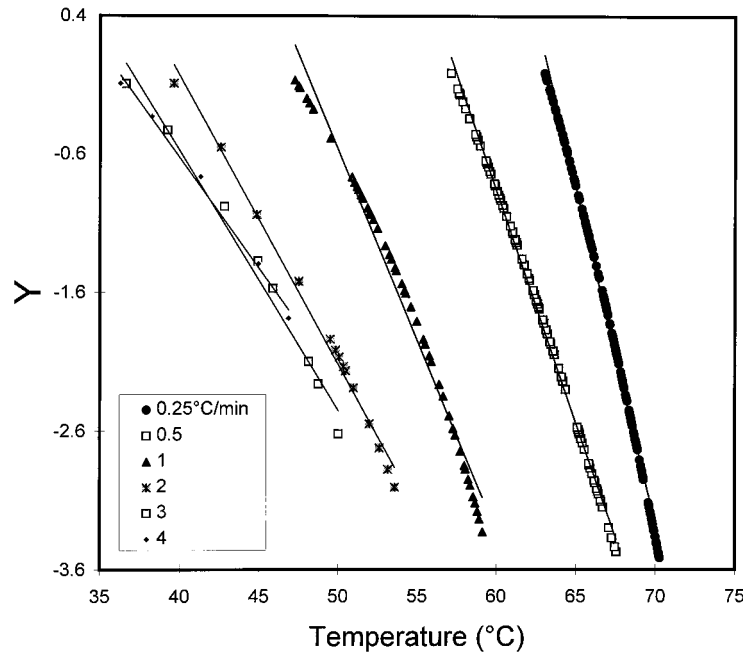
Figure 14 Linear plots of $Y = \ln[-\ln(1 - X_V)]$ against temperature for dyed PDS with cooling rate as a parameter.

duced as the cooling rate was increased from 1 to 2°C/min (almost 60% change!) as was illustrated earlier in Figure 11. A continuously diminishing crystal content observed in samples at even higher rates would, in our opinion, strongly affect the kinetic calculations based on this method. To overcome this problem, one could either take into consideration only the lowest cooling rate domain or seek complementary information utilizing a technique where a lower-speed process is not an obstacle (i.e., hot-stage microscopy). Finally, it is worth mentioning that due to the very slow crystallization of the copolymer only two data points were attainable (at 0.25 and 0.5°C/min), generating the Avrami exponent of 3.39.

Table IV Characteristic Kinetics Parameters Determined from Figure 14

Cooling Rate (°C/min)	a	Intercept $(-a \times T_q)$	T_q (°C)
0.25	−0.498	31.5	63.3
0.5	−0.339	19.5	57.4
1	−0.275	13.2	48.0
2	−0.211	8.43	40.0
3	−0.187	6.89	36.8
4	−0.160	5.76	36.0

CONCLUSIONS

DSC was used to study the crystallization behavior in PDS-based materials. Kinetic analyses were performed for isothermal and nonisothermal crystallization under controlled heating and cooling rates.

A classical Avrami approach was used to evaluate important kinetic and morphological parameters during isothermal crystallization of these materials. For that purpose, a partial integration under a heat flow–time curve was used to calculate the crystal fraction volume developed at a given time. Based on the determination of half-time crystallization, the maximum rate of the process for undyed and dyed PDS was found to occur around 45°C. The Avrami exponent, n, for these two polymers was determined to be around 2.5, indicating the heterogeneous nucleation with three-dimensional diffusion-control spherulitic growth. The crystallizability and crystallization rate of the 89/11 PDS/glycolide copolymer was found to be significantly reduced compared to those of the PDS homopolymers. The reason for this behavior is a disruptive role that the glycolic acid comonomer plays in the overall ability of the copolymer's macromolecular chains to align properly for the crystal formation.
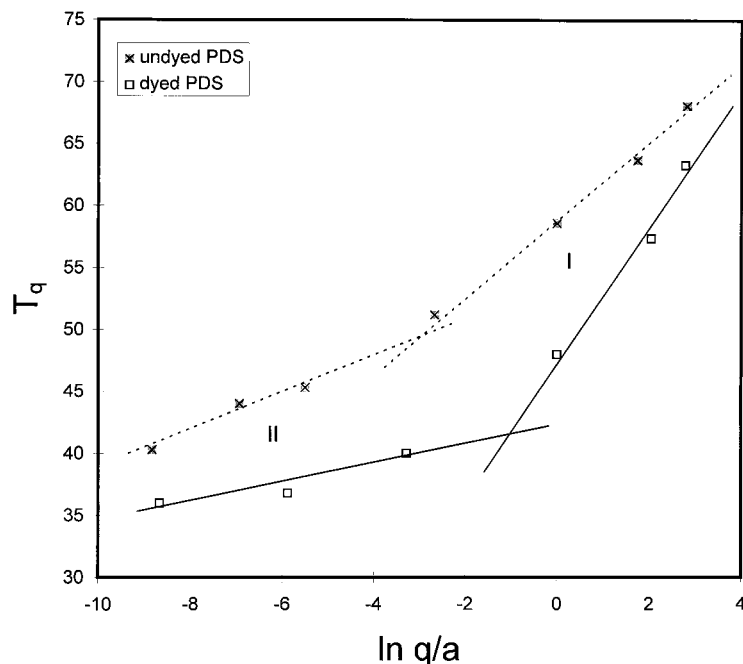
Figure 15 Determination of Avrami exponent, n, using linear plots of T_q against ln q/a for undyed and dyed PDS samples.

A secondary crystallization phenomenon was identified in all studied materials that sets in around 70°C during nonisothermal crystallization runs from the quenched state at constant heating rates. It was shown that secondary crystallization markedly influenced the final crystallinity extent, as well as the overall rate of crystallization. On close examination, we found that secondary crystallization is also present in the later stages of both the constant cooling rate nonisothermal processes and the isothermal processes above 60°C.

Finally, an attempt was made to use the Ozawa approach and the recently proposed Calculus method to describe the crystallization kinetics of PDS polymers during cooling from the melt at constant cooling rates. Although we were able to calculate the apparent values of the Avrami n using the Ozawa approach, we found that the calculated values were dependent on the temperature, inconsistent with the theory. On the other hand, using the Calculus method, we arrived at two distinct values of the Avrami exponent depending on the cooling rate employed. We believe that the values obtained at lower cooling rates are legitimate and those obtained at higher rates lead to artifactual inaccuracies. This is due to DSC's insensitivity to account properly for the critically low crystallinity observed at higher cooling rates.

Thus, the Ozawa method and the Calculus method for nonisothermal cooling processes should be used with care.

REFERENCES

1. Meares, P. In The Fusion and Crystallization of Polymers; D. Van Nostrand: New York, 1967; Chapter 5.
2. Wunderlich, B. Macromolecular Physics; Academic: New York, 1976; Vol. 2.
3. Tong, H. M.; Chou, N. J.; Saraf, R. F.; Kowalczyk, S. P. In Polymer Structures and Synthesis Methods; Butterworth-Heinmann: Stoneham, MA, 1994; Chapter 1.
4. Misra, S.; Lu, F.-M.; Spruiell, J. E.; Richeson, G. C. J Appl Polym Sci 1995, 56, 1761.
5. Nicolais, L. J Appl Polym Sci 1997, 64, 911.
6. Goldfarb, L.; Garrett, T. B.; Rittenhouse, J. R.; Messersmith, D. C. Makromol Chem 1974, 175, 2483.
7. Hay, J. N.; Mills, P. J. Polymer 1982, 23, 1380.
8. Marega, C.; Marigo, A.; Noto, V.; Zannetti, R. Makromol Chem 1992, 193, 1599.

9. Phillips, P. J.; Rensch, G. J.; Taylor, K. D. J Polym Sci Part B Polym Phys 1987, 25, 1725.

10. Yu, T. J.; Chu, C. C. J Biomed Mater Res 1993, 27, 1329.

11. Ward, I. M.; Hadley, D. W. An introduction to the Mechanical Properties of Solid Polymers; Wiley: New York, 1993.

12. Ezquerra, T. A.; Majszczyk, J.; Balta-Calleja, F. J.; Lopez-Cabarcos, E.; Gardner, K. H.; Hsiao, B. S. Phys Rev B 1994, 50, 6021.

13. Stein, R. S.; Misra, A. J Polym Sci Part B Polym Phys 1972, 11, 109.

14. Lu, F.; Spruiell, J. E. J Appl Polym Sci 1987, 34, 1541.

15. Bulkin, B. J.; Lewin, M.; DeBlase, F. J. Macromolecules 1985, 18, 2587.

16. Bezwada, R. S.; Jamiolkowski, D. D.; Cooper, K. In Handbook of Biodegradable Polymers; Domb, A. J.; Kost, J.; Wiseman, D. M., Eds.; Harwood: Singapore, 1997; Chapter 2.

17. Doddi, N.; Versfelt, C.; Wasserman, D. U.S. Patent 4 052 988, 1977 (to Ethicon, Inc.).

18. Erk, M. K.; Basyigit, I.; Kolbakir, F.; Keceligir, T.; Yilman, M. Vasc Surg 1995, 29, 209.

19. Fatou, J. M. G.; Barrales-Rienda, J. M. J Polym Sci 1969, 7, 1755.

20. Migliaresi, C.; Lollis, A. D.; Fambri, L.; Cohn, D. Clin Mater 1991, 8, 111.

21. Migliaresi, C.; Cohn, D.; Lollis, A. D.; Fambri, L. J Appl Polym Sci 1991, 43, 83.

22. Urbanovici, E.; Schneider, H. A.; Brizzolara, D.; Cantow, H. J. J Therm Anal 1996, 47, 931.

23. Iannace, S.; Nicolais, L. J Polym Sci Part B Polym Phys 1997, 35, 911.

24. Chu, C. C. Polymer 1980, 21, 1480.

25. Avrami, M. J Chem Phys 1940, 8, 212.

26. Brandrup, J.; Immergut, E. H., Eds.; Polymer Handbook, 3rd ed.; Wiley: New York, 1989.

27. Physical Properties of Polymers Handbook; Mark, J. E., Ed.; American Institute of Physics: Woodbury, NY, 1996.

28. Ozawa, T. Polymer 1971, 12, 150.

29. Cazé, C.; Devaux, E.; Crespy, A.; Cavrot, J. P. Polymer 1997, 38, 497.

30. Chuah, K. P.; Gan, S. N.; Chee, K. K. Polymer 1998, 40, 253.

31. Dolegiewitz, L., unpublished data.